N82 28717

5.6   GEOMETRIC AND RADIOMETRIC DISTORTION IN
       SPACEBORNE SAR IMAGERY*

J.C. Curlander

Jet Propulsion Laboratory
California Institute of Technology
4800 Oak Grove Drive
Pasadena, California 91109

I. INTRODUCTION

Synthetic aperture radar (SAR) [1,2] is a side-looking sensor capable of
very fine along-track resolution. This characteristic, in addition to its
all-weather monitoring capability, makes it an attractive instrument for
generating space imagery. A SAR typically operates in a spectral region
(1-10 GHz) that complements most optical scanners (LANDSAT). In this region,
the subsurface sensing depth is much greater and the reflectance properties
of imaged terrain objects are different [3]. A SAR will therefore collect a
complementary set of "terrain signatures" that when registered with other
spectral data can greatly facilitate the interpretation of remotely sensed
imagery. But before multisensor data can be properly registered, the various
types of distortion inherent in SAR imagery must be quantitatively analyzed.
This requires an understanding of the properties of the sensor as well as the
data processing system used in the image formation.

The production of quality imagery from spaceborne SAR data requires
extensive processing of the raw echo data. This procedure is more complex
than previously used for aircraft SAR imagery due to the large increase in
sensor altitude. The correlation procedure must compensate not only for
undesirable spacecraft motion, but also for target motion resulting from
Earth curvature and rotation [4,5]. To simplify this procedure,
approximations are often made that can result in both geometric and
radiometric distortion in the image product. Furthermore, the viewing
geometry of the SAR and the characteristics of the data collection system
will also introduce distortion into the imagery. Precise registration of SAR
imagery with other types of remotely sensed imagery requires the

identification of these distortions and the development of post-processing

techniques to rectify them. Furthermore, considering the large quantity of

data, it is desirable that these post-processing techniques be automated and

designed to interface directly with the image processor to generate a

geometrically and radiometrically correct product without supervision or

operator interaction.

This paper will summarize what is currently known about these

distortions and describe the development to date of unsupervised

post-processing rectification techniques. The geometric distortion can be

divided into two categories. The first catagory consists of distortion

derived from the radar viewing geometry. This includes such effects as

ground range nonlinearities, radar foreshortening and radar layover. The

second category consists of distortions introduced during the data

processing. These distortions result from approximations made during the

correlation such as in estimation of the target phase history, or

compensation for the earth rotation. The processor induced distortions will

obviously depend on the specific correlation algorithm used for image

formation. This paper generally addresses the effects on the image product

resulting from assumptions during the processing and it specifically

considers distortions inherent in digital imagery produced by the digital

image processor at JPL [6].

II. SAR REVIEW

This section is intended as a brief tutorial on SAR system

characteristics and processing techniques. Basic system parameters are

introduced that are relevant to understanding the sensor and processor

induced distortion to be discussed in subsequent sections. Interested

readers will find an excellent treatment of various characteristics of SAR in

a recently published collection of papers [7].

2.1 SAR Sensor Characteristics

The viewing geometry for a SAR in the imaging mode is illustrated in

Figure 1. The sensor moves along a predetermined orbit track radiating

energy in the form of pulses and receiving the backscattered signal. This

data is either recorded on film for later optical processing or is

transmitted on a downlink to a tracking station where it is digitized and

recorded on high-density tape for digital processing. The antenna pointing

direction is normal to the flight path and its orientation with respect to

the spacecraft is normally fixed. Two important system parameters are the

antenna look angle θ, defined as the angle of the antenna beam with respect

to nadir direction, and the slant range R, the distance from the sensor to the

imaged target area. The radar antenna range beamwidth β_r and the

spacecraft altitude H, determine the cross-track dimension of the radar

footprint.

The radar transmitter is typically designed to operate in a frequency

region between L-band and X-band, thus permitting cloud and fog penetration.

The pulse repetition frequency (PRF) of the radar and the spacecraft velocity

determine the azimuth (along-track) resolution. This is typically designed

to be several times higher than the range (cross-track) resolution so that the azimuth return can be divided into several looks for incoherent summation to reduce the speckle noise. The range resolution is determined by the spectral bandwidth of the transmitted pulse. Coded pulses such as a chirp waveform are typically used to achieve the maximum resolution for a given level of transmitter power [8]. During the image processing these pulses must be compressed to a point response. Imperfect compression can result in both reduced resolution and range sidelobes in the image.

2.2 SAR Processor Characteristics

Processing raw echo data into finished imagery essentially consists of the following four steps (16):

    (1) Range pulse compression;

    (2) Doppler parameter estimation;

    (3) Azimuth correlation; and

    (4) Speckle reduction.

2.2.1 Range Pulse Compression

The purpose of this step is to compress the time dispersed radar transmitted pulse into an impulse. A chirp function is the radar pulse waveform typically used because of its focusing capability in an optical SAR processor. The key to attaining an adequate signal-to-noise ratio is transmission of a wide-band pulse and use of the data processor to compress this pulse. The range resolution can be approximated by

$$\rho_R = \frac{c}{2W} \qquad (1)$$

167

where c is the speed of light and W is the pulse bandwidth. Spaceborne SAR requires unusually large pulse compression ratios compared with aircraft radar to achieve fine image quality.

2.2.2 Doppler Parameter Estimation

Formation of the synthetic aperture is critically dependent on accurate estimation of the phase delay history of the return echo signal. This phase delay can be approximated by [9]

$$\phi(t) = \phi(0) + 2\pi\left(f_d t + \frac{1}{2} \dot{f}_d t^2\right) \tag{2}$$

where $\phi(0)$ is the phase at t=0, f_d is the Doppler frequency shift of the echo data, and $\dot{f}_d$ is the Doppler rate, both evaluated at t=0. These two parameters, f_d and $\dot{f}_d$, can be estimated based on the orbit and attitude data. If an accurate ephemeris is not available, these estimates can be used as initial predicts and further refined by evaluation of certain characteristics in the resultant imagery. Details of these refinement techniques, termed autofocusing for $\dot{f}_d$ and clutterlock for f_d, can be found in the literature [9,10].

2.2.3 Azimuth Correlation

One of the primary features of SAR is its very high resolution. As previously discussed, fine range resolution is achieved by transmission of a wide bandwidth pulse and compression of this pulse in the data processor. A high azimuth resolution is achieved by coherent processing of echo data from

successive radar pulses. The azimuth correlation operation essentially
simulates a very narrow effective beamwidth in the azimuth direction by
coherently adding the returns of several radar echoes. This operation is
performed on range compressed data and involves shifting the phase reference
function given in (2) and summing the resultant detected echo data.

The complexity of the azimuth correlation is increased by the range
migration of the target as it passes through the antenna beam. This
migration consists of a range walk term which is directly proportional to the
elapsed along-track time and a range curvature term, which is proportional to
the square of the along-track time. To compensate for the fact that the
target transverses may range resolution elements, the input data is resampled
before the phase reference function is applied. After phase detection, the
return from each pulse over the length of the synthetic aperture is summed to
obtain a refined estimate of the target's brightness. If the returns are
added over the full aperture, a single-look full resolution image is
produced. If the aperture is divided into sections, several single-look
reduced resolution images are produced. For example, two single-look images
can be produced by dividing the phase reference function in half and
processing the first and second portions of the target response separately.
The single-look images are then added incoherently as described in the next
section to obtain a multiple-look image.

2.2.4 Speckle Reduction

Coherent processing of radar echo data is used to achieve very fine
along-track resolution, but this same processing also makes the images

169

susceptible to speckling effects. Basically, speckling results from scattering of non-uniformly distributed reflectors within a resolution cell during the period the cell is within the antenna beam. The speckles are signal dependent and therefore act like multiplicative noise. Techniques for speckle suppression essentially fall into two main categories: 1) averaging several reduced resolution images produced from independent looks; and 2) filtering a full-resolution single-look image to smooth the speckle.

The multiple-look overlay technique is typically used for image production because it can achieve a satisfactory level of speckle reduction with a minimal amount of additional computation [11]. To produce multiple looks, the phase reference function is divided into segments during azimuth correlation. Each segment is applied to the appropriate portion of the return echo data to produce a reduced resolution single-look image of the target area. The single look imagery is then registered and averaged to produce a multi-look product with reduced speckle noise.

The speckle can also be reduced by filtering a single-look high resolution image [12]. Smoothing algorithms have been devised based on the local statistics of the noise. In general, these filters can achieve a greater speckle reduction for a given resolution product then the multiple-look overlay technique, but because of the additional computational load, this approach is not feasible for large-scale image production.

C - 3

III. GEOMETRIC DISTORTION

SAR imagery is subject to several types of geometric distortion that must be corrected before the imagery can be properly registered with other sensor data. These distortions can be classifed into two main categories: 1) sensor derived distortion, and 2) processor derived distortion.

3.1 Sensor Derived Distortion

The geometric distortions classified in this category are mainly derived from the viewing geometry of the radar. Design parameters such as the sensor altitude, look angle, and range beamwidth are critical in determining the degree of distortion in the imagery. In most cases, post-processing will be required to correct these distortion effects.

3.1.1 Ground Range Nonlinearity

Perhaps the most predominant distortion in a spaceborne SAR image is the ground range nonlinearity. This effect results from the fact that each pixel represents a constant slant range distance rather than uniform ground spacing. Figure 2 illustrates the type of distortion inherent in a slant range projection. Features in the near range of a slant range image are compressed with respect to the far range. For example, a circle in the far range would have the appearance of an ellipsoid in the near range of the image. To project the image in a ground range format, the ground distance represented by each pixel in the slant range projection must be determined from

$$\Delta x = \frac{\Delta r}{\sin \phi} \qquad (3)$$

where Δr is the slant range pixel spacing and ϕ is the incidence angle of the radar beam at the target. The slant range spacing is constant and is given by

$$\Delta r = \frac{c}{f_s} \tag{4}$$

where c is the speed of light and f_s is the sampling frequency. The maximum frequency is limited by the range bandwidth. For SEASAT SAR, this frequency was 45.53 MHz producing a slant range spacing of 6.59 m.

The incidence angle, ϕ, can be related to the beam elevation angle, θ, by trigonometric means as follows (Figure 3)

$$\phi = \sin^{-1} \left[\frac{(H + R_e) \sin \theta}{R_e} \right] \tag{5}$$

where R_e is the radius of the earth, H is the spacecraft height and θ, the look angle, is given by

$$\theta = \cos^{-1} \left[\frac{R^2 + (H + R_e)^2 - R_e^2}{2R(H + R_e)} \right] \tag{6}$$

The relationships for ϕ and θ in (5) and (6) have been derived assuming a smooth spherical surface with a radius equal to the radius of the earth at the target. Since the incidence angle is a function of the terrain, equation (5) is ony approximate for a rough surface. This could result in an error in the ground range projection.

172

3.1.2 Radar Foreshortening [13]

Radar foreshortening is the variation in apparent size of identical features at different slopes with respect to the sensor. The effect for terrain sloping toward the radar is an increase in the effective incidence angle. Terrain sloping toward the radar will therefore appear elongated with respect to terrain sloping away from the sensor. This is illustrated in Figure 4. Since terrain features are recorded as a function of the slant range distance from the sensor, slope ab is mapped into a'b' in the image plane while bc is mapped into b'c'. Although ab and bc are identical in length, b'c' will be more than three times larger than a'b' in the image. Quantitatively stated the elongation (or shortening) factor is given by

$$\frac{a'b'}{ab} = \sin(\theta - \beta_s) \qquad (7)$$

$$\frac{b'c'}{bc} = \sin(\theta + \beta_s) \qquad (8)$$

where β_s is the surface slope and θ is the look angle. Thus for a look angle similar to the terrain slope, the foreshortening effect is most severe.

The foreshortening can be corrected if the radar altitude and look angle are known and a terrain map of the target area is available. One technique to correct the foreshortening is as follows [14]: A digital topographical map is illuminated from the same angle that the radar used to generate the original foreshortened image. This can be routinely done using a radar simulation program. The resultant movement of each pixel in the simulated image is recorded. This image is then registered to the actual radar image

and the inverse of this movement is applied. The result of this type of process is shown in Figure 5. Note that the presence of certain geological features becomes readily apparent. This technique, although capable of producing an image without foreshortening, is a tedious process which requires exact registration of the simulated image with the actual radar image. In addition, this technique requires a priori terrain information for the imaged area which may not be available.

3.1.3 Radar Layover [13]

Radar layover is a distortion inherent in all radar imaging of irregular terrain. It results from an image pixel being placed in its cross-track location based on its range from the sensor. If the target area contains features with steep slopes, the top of the feature can be at a closer range than the bottom. This effect is shown in Figure 6. It is especially severe when features of appreciable level relief appear in the near range.

3.1.4 Earth Rotation

The earth rotation effect is common to satellite scanning systems where the scan lines are gathered serially in time while the earth's surface is rotating during the imaging period. This results in the near edge of the image being skewed with respect to the nadir track of the satellite as shown in Figure 7a. This effect, known as range walk or range migration can be compensated by resampling the echo data during the image processing. Figure 7b shows the outline of an image frame after data resampling to compensate for the range walk. The stairstep edge is an artifact of the multiple-look overlay process and does not result in any discontinuities within the frame.

3.2 Processor Derived Distortion

The distortions generated during image formation are obviously dependent on the specific processing algorithm. Generally, approximations made in determining the phase reference function will result in a skewed image. This section discusses some typical approximations and the resultant distortions.

3.2.1 Earth Curvature and Rotation

In the previous section, the range walk effect that results from the Earth rotation was described. This rotation in conjunction with the Earth curvature can also result in an image skew in the azimuth direction. This skew occurs during the image formation process. As previously discussed, to process raw echo data into imagery the Doppler frequency and frequency rate must be determined. The rotation and curvature of the earth, however, result in a complex Doppler response that is a function not only of target latitude but also depends on target position within the swath. A plot of Doppler frequency as a function of swath position and latitude is sh own in Figure 8. It is extremely difficult to design a processor that adapts to the varying frequency without introducing reduced image resolution resulting from misregistration during the multiple-look overlay. As an alternative to precise tracking of the Doppler frequency during the processing, an optimum f_d is selected for the entire image frame and the resultant skew is corrected in the post-processing. This skew resulting from the Doppler mismatch is essentially in the azimuth direction as shown in Figure 9. The amount of skew is dependent on the difference between the actual Doppler response of each target and the f_d used in the processing and is given by

$$\Delta N_{az} = \frac{\Delta f_d}{f_d} \cdot \frac{PRF}{L} \tag{9}$$

175

where PRF is the pulse repetition frequency, L is the number of looks, Δf_d is the Doppler frequency mismatch, $\dot{f}_d$ is the Doppler rate and ΔN_{az} is the azimuth displacement in pixels. Note that since the iso-Doppler lines are nearly linear, a linear correction can be used to deskew the image. For a 100 km swath width as in SEASAT SAR, a typical skew is $\Delta N_{az} \simeq 150$ pixels or 2.5 km, which corresponds to a skew angle of 1.5 degrees.

3.2.2 Sensor Parameter Shift

The eccentricity of the spacecraft orbit requires adjustment of the sensor parameters at certain intervals during the orbit. This can result in either a discontinuity, or variation of the pixel resolution within an image frame. A sharp discontinuity in the image results from a shift in the delay of the pulse sampling window. This parameter shift is made in the data collection system to maintain the optimum signal-to-noise ratio in the sampled echo data. If the pulse sampling window were not adjusted as the spacecraft altitude changed, this window would not center on the portion of the signal with the strongest return and the resulting imagery would be degraded. The effect on an image produced from data collected during a sampling window shift is to displace one part of the image in range with respect to the other, resulting in a line of discontinuity across the frame.

Another parameter requiring adjustment based on variation in the spacecraft orbit is the pulse repetition frequency (PRF). The PRF is adjusted to prevent pulse mixing or range ambiguities. An upper limit on the PRF is set to avoid interference between successive pulses. This limit is dependent on the range swath width which is in turn a function of spacecraft altitude. A lower limit on the PRF is determined by the resolution and

176

azimuth ambiguity requirements. This bound is also dependent on the spacecraft orbit. To keep the PRF within these bounds, it must be adjusted according to variation in the spacecraft height. Certain frames therefore may contain pixels of mixed resolution if the PRF was adjusted during that frame's data collection period.

3.3 Radiometric Characteristics

Registration of a SAR image to an optically sensed image or another SAR image can present a difficult problem since the apparent brightness of an image pixel is critically dependent on the relative position of the sensor. A small change in the aspect angle can significantly alter the appearance of a scene as shown in Figure 10. Furthermore, SAR imagery is corrupted by both speckle and thermal noise, pulse compression sidelobes, ambiguity responses and weak signal suppression effects [6]. With proper radar and processor design, the effects of most of these distortions on the final image product can be minimized. The image degradation resulting from speckle noise is greatest in coherent imagery of terrain with a surface roughness comparable to the wavelength of the illumination [15]. The speckle can be reduced by summarion of looks or filtering at the cost of pixel resolution.

When attempting to register SAR imagery from two adjacent passes for the purpose of constructing a mosaic, the distortion resulting from speckle can cause misregistration. This results from the fact that for a small change in the sensor position (4 km for SEASAT) the speckle noise in the resultant imagery is totally independent. Therefore, from one pass to the next a feature may be distorted differently resulting in a poor correlation between the two frames. An additional factor that can cause image misregistration between two adjacent passes is a phenomenon called specular point

177

migration illustrated in Figure 11. This effect occurs when a feature with a
varying slope is imaged from two different sensor positions. The apparent
position of a feature changes relative to other features within the frame
because the point of maximum reflectivity of that feature occurs at a slope
perpendicular to the radar beam. This effect can also result in apparent
misregistration of features in SAR imagery.

IV. CURRENT PROGRESS IN REGISTRATION/RECTIFICATION OF SAR FREQUENCY

Many of the geometric and radiometric distortions present in digitally processed SAR imagery do not occur in optically sensed imagery. The effect of these distortions on image resolution, rectification and ultimately mosaicking have not been fully investigated. To date very few mosaics have been constructed with digital SAR imagery and at present no comprehensive studies have been conducted to investigate the feasibility of generating unsupervised mosaics.

The SAR processing research group at Jet Propulsion Laboratory has laid the ground work for development of an unsupervised mosaicking procedure and plans to implement this procedure within the next year. Recently completed is an algorithm capable of determining the absolute location of an image pixel without the aid of ground reference points [6]. This algorithm utilizes information provided by the spacecraft ephemeris and characteristics of the sensor data collection system to predict the latitude and longitude of an arbitrary image pixel. Tests have shown this technique has an accuracy of better than 200 m for SEASAT SAR data. The target location uncertainty is primarily dependent on the accuracy of the spacecraft position and velocity provided by the ephemeris and the validity of the assumed geoid in the target area.

The capability for unsupervised pixel location is a prerequisite for automated rectification and mosaicking of SAR imagery. With informtion on both the sensor and target position, the parameters for slant range to ground-range conversion can be determined as well as the Doppler shift in the echo

data. Using this information and the image processing parameters, it is a
simple procedure to conduct range and azimuth interpolation to remove the
ground range nonlinearity and azimuth skew distortions. An algorithm has
been developed at JPL to correct these distortions for digitally cor- '   d
SEASAT imagery. A preliminary version of this algorithm has been   plement
utilizing the hardware architecture of the digital processor. This hardware
configuration, shown in Figure 12, was designed both for efficiency and
economy [17]. The host computer is a Systems Engineering Laboratory 32/77
which features very rapid I/O data transfers. Attached to the host are three
Floating Point Systems AP120b array processors and four 300 Mbyte discs. The
image data is transferred from disc to the array processors through the
host. Each AP operates simultaneously on a separate area of the image and
returns the rectified product to the host to be merged and transferred to
disc. It is anticipated that with proper design this approach can rectify a
6000 x 6000 pixel frame which covers a 100 x 100 km ground area in under
30 minutes. This approach is compatible with the image processor and could
be easily incorporated into the image production procedure.

A preliminary version of this algorithm is curr--tly operating at JPL.
It utilizes a single AP and makes some simplifying assumptions in generating
the rectification parameters. The current operating time for a full   frame
is 80 minutes. The output has been resampled to 12.5 m spacing in both the
range and azimuth dimensions. As a result of approximation, the rectified
product still contains some residual skew. Tests show approximately a 200 m
registration error across a 100-km frame. The expected registration error
using a more exact version of the algorithm is less than 50 m or about
2 pixels.

180

Following completion and test of the rectification algorithm, studies are planned to investigate the feasibility of generating unsupervised image mosaics. Imagery from parallel passes as well as ascending and descending passes will be examined. Statistics will be compiled on the correlation of common features as well as the misregistration between geometrically corrected images from two adjacent passes. Automated feature detection techniques are also being considered to locate suitable tie points.

Obviously much work remains to be done with regard to rectification and registration of SAR imagery. It is clear that digitally correlated imagery offers distinct advantages over optical imagery such as: reproducible processing, large inherent dynamic range and highly accurate pixel location. The refinement of these techniques utilizing SEASAT SAR data will provide insight into the design of future sensor systems to optimize the registration and rectification accuracy.

ACKNOWLEDGEMENT

REFERENCES

[1] L.J. Cutrona, "Synthetic Aperture Radar," Radar Handbook M.I. Skolnik, ed., McGraw-Hill, New York, 1970, Chapter 23.

[2] W.M. Brown and L.J. Procello, "An Introduction to Synthetic Aperture Radar Theory," IEEE Spectrum, pp 55-62, Sept. 1969.

[3] J.D. Lent and G.A. Thorley, "Some Observations on the Use of Multiband Spectral Reconnaissance for the Inventory of Wildland Resources," Remote Sensing of the Environment, Vol. 1, pp 31-46, 1969.

[4] J.C. Kirk, "A Discussion of Digital Processing in Synthetic Aperture Radar," IEEE Trans on Aero and Elec Systems, Vol. AES-11, No. 3, pp 326-337, May 1975.

[5] C. Wu, "A Digital System to Produce imagery from SAR Data," AIAA System Design Driven by Sensors Conference, Paper No. 76-968, Pasadena, California, Oct. 1976.

[6] C. Wu, B. Barkan, B. Honeycutt, C. Leary and S. Pang, "An Introduction to the Interim Digital SAR Processor and the Characteristics of the Associated SEASAT SAR Imagery," Publication 81-26, Jet Propulsion Laboratory, Pasadena, Calif, Apr. 1981.

[7] J.J. Kovaly, ed., Synthetic Aperture Radar, Artech House, Inc., Dedham, Mass., 1978.

[8] C.E. Cook and M. Bernfeld, <u>Radar Signals</u>, Academic Press, New York, 1967.

[9] J.C. Curlander, C. Wu, D. Held and F. Li, "Estimation of Doppler Parameters for Spaceborne Synthetic Aperture Radar Processing," in preparation.

[10] R.E. Morden, F. Powell, "SAPHIRE Design and Development," Paper GERA-2177, Rev. A, Goodyear Aerospace Corp., Arizona Division, Litchfield Park, Arizona, Sept. 1977.

[11] L.J. Porcello, N.G. Massey, R.B. Innes, J.M. Marks, "Speckle Reduction in Synthetic Aperture Radars," <u>Journal of the Optical Society of America</u>, Vol. 66, No. 11, pp 1305-1311, Nov. 1976.

[12] J.S. Lee, "Speckle Analysis and Smoothing of Synthetic Aperture Radar Images," <u>Computer Graphics and Image Processing</u>, Vol. 17, pp 24-32, 1981.

[13] A.J. Lewis and H.C. MacDonald, "Interpretive and Mosaicking Problems of SLAR Imagery," <u>Remote Sensing of the Environment</u>, Vol. 1, pp 231-237, 1970.

[14] M. Naraghi, W. Stromberg and M. Daily, "Geometric Rectification of Radar Imagery Using Digital Elevation Models," submitted to <u>Photogrametric Engineering and Remote Sensing</u>.

[15] J.C. Dainty, ed., <u>Laser Speckle and Related Phenomena</u>, Springer-Verlag, Berlin, 1975.

[16] J.C. Curlander and W.E. Brown, Jr., "A Pixel Location Algorithm for Spaceborne SAR Imagery," <u>Proceedings of the 1981 International Geoscience and Remote Sensing Symposium</u>, Washington, D.C., pp 843-851, June 1981.

[17] C. Wu, B. Barkan, W. Karplus, and D. Caswell, "SEASAT Synthetic Aperture Radar Data Reduction Using Parallel Programmable Array Processors," <u>Proceedings of the 1981 International Geoscience and Remote Sensing Symposium</u>, Washington, D.C., pp. 541-548, June 1981.
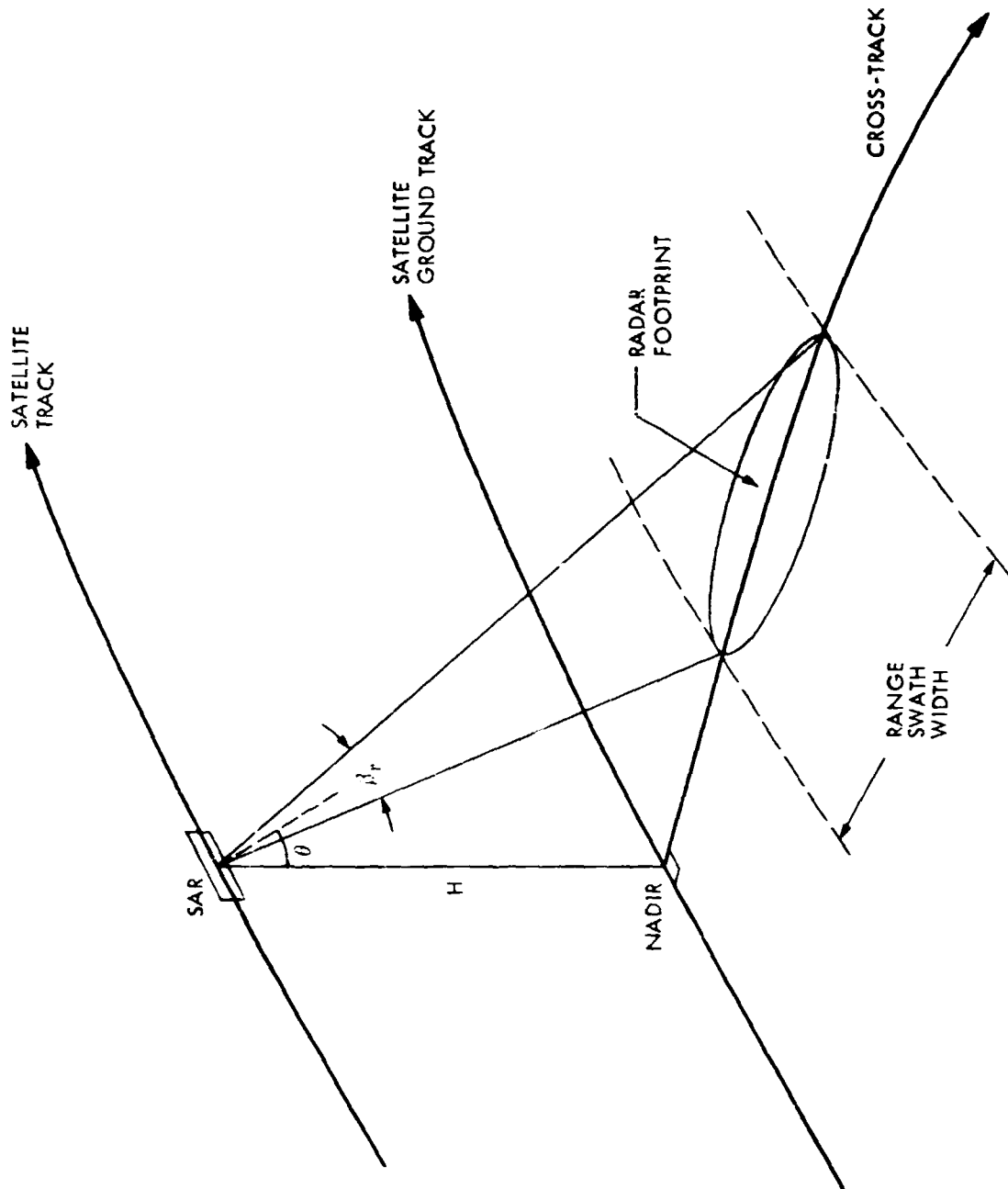
Figure 1. Viewing geometry for a typical side-looking synthetic aperture radar
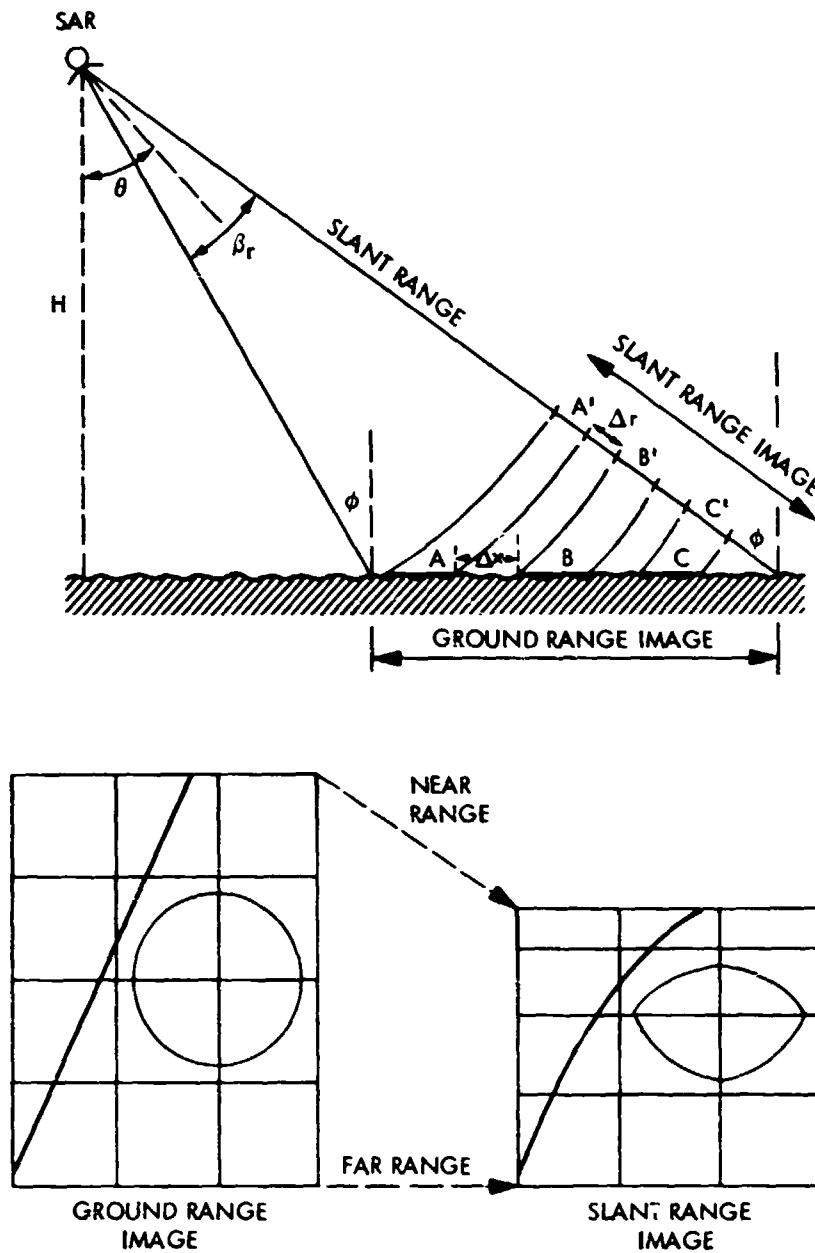
Figure 2. Slant range to ground range nonlinearity inherent
in all side looking radar systems. Near range
features are compressed relative to far range
features because of change in incidence angle, φ.

187
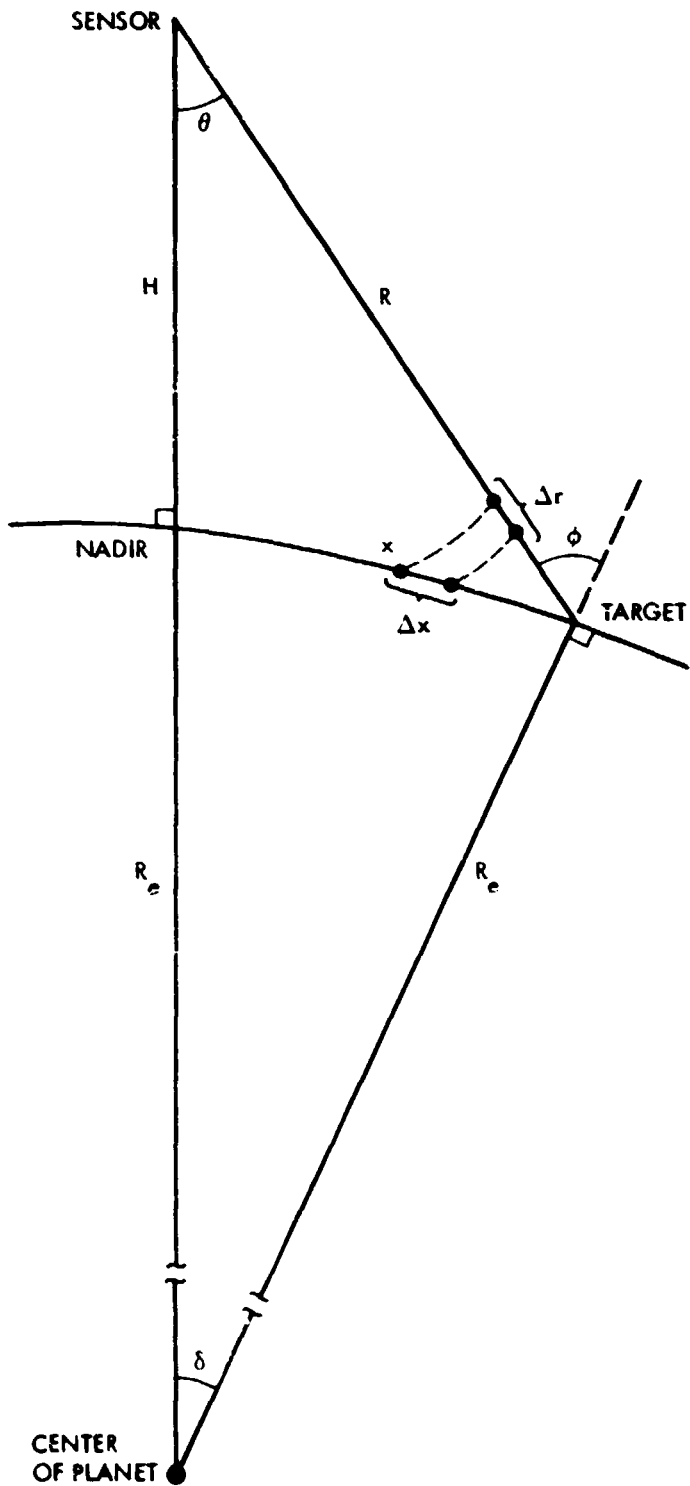
Figure 3.   Relationship between look angle, θ and incidence
angle φ for a smooth spherical planet surface.
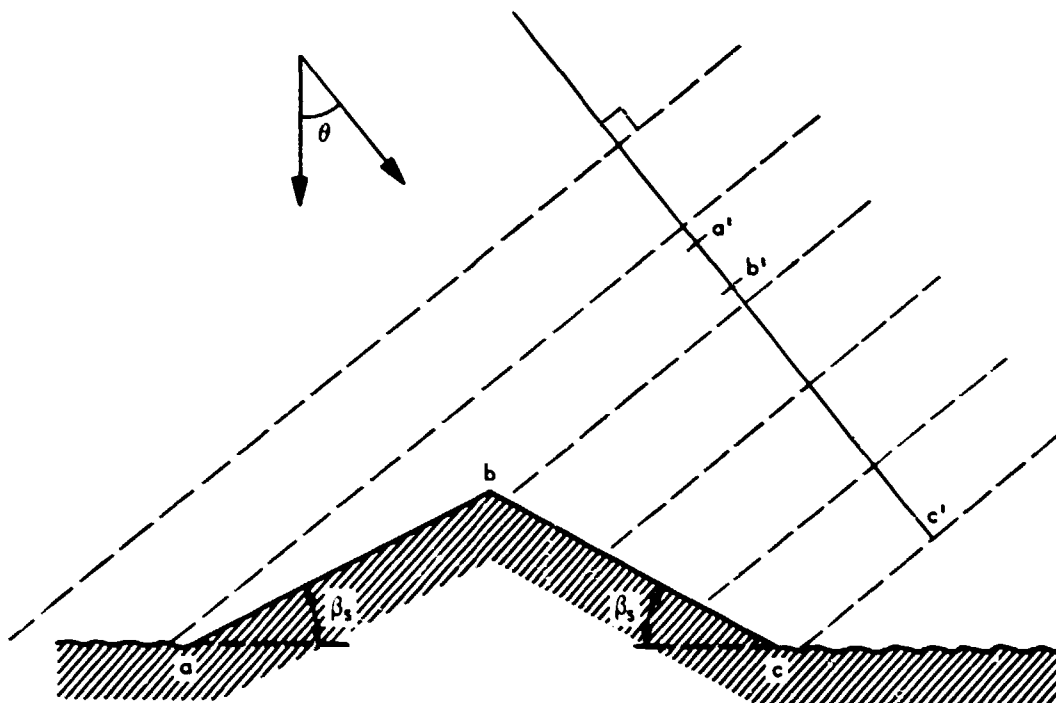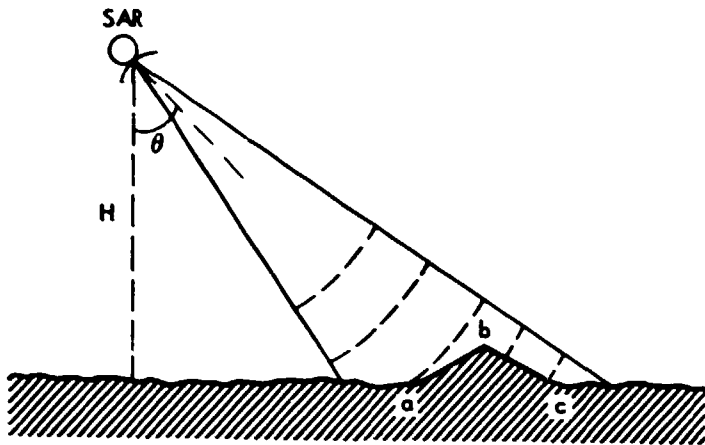
Figure 4. The radar foreshortening effect causes slopes inclined toward the radar to appear shorter than those inclined away from the radar.

a

b
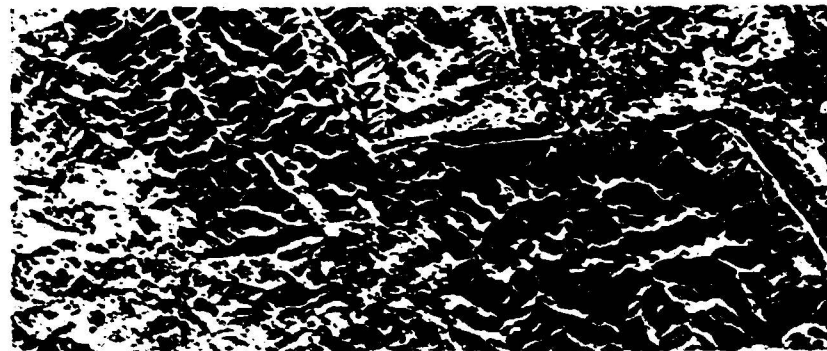
c

Figure 5.   Results of compensation for radar foreshortening using
            digital terrain model.   a) Simulated radar image from
            topographical map, b) Corrected SEASAT image, c) Origi-
            nal SEASAT image.   Note the enhancement of fault lines
            not evident in original image (Naraghi, 1981).

190
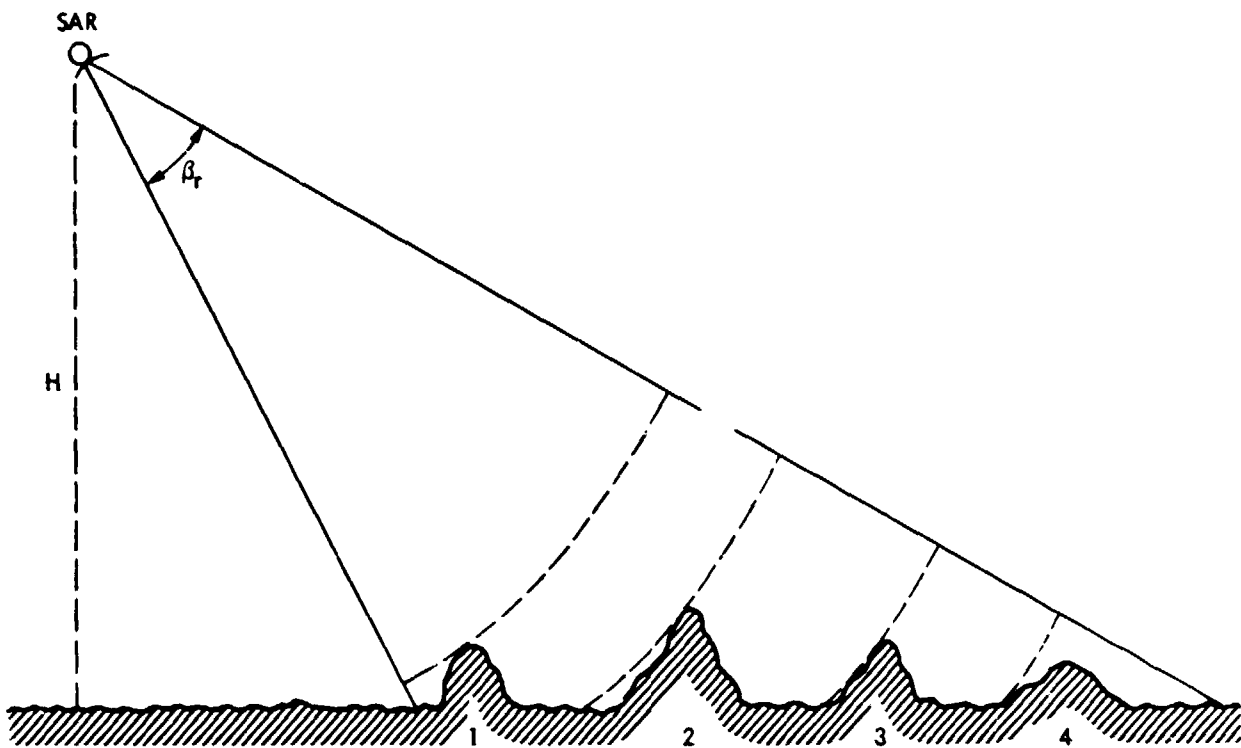
Figure 6. Radar layover is a function of the terrain
slope and the slant range to the target. Layover
occurs when the surface feature slope exceeds the
look angle. Signal scattered from the top of
features 1 and 2 will be placed at a nearer cross-
track position in the image than signal scattered
from the bottom.
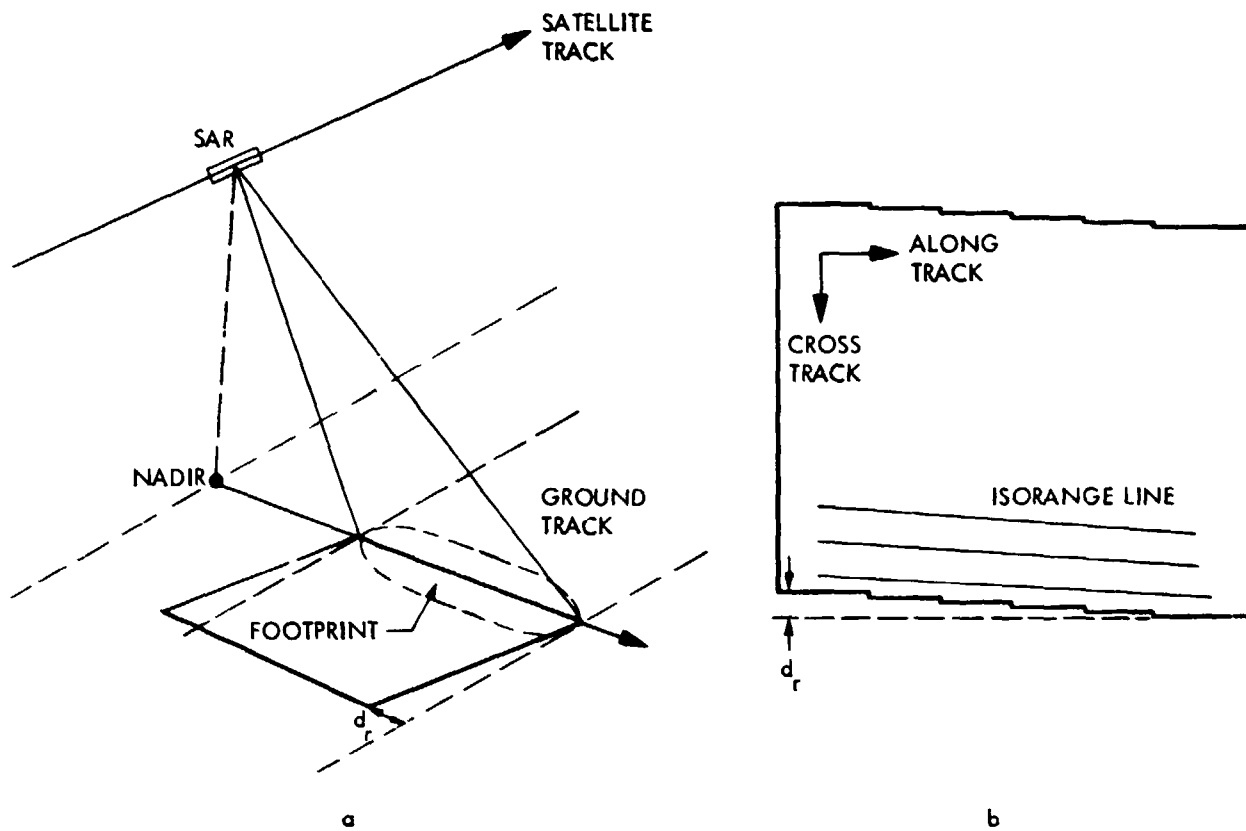
Figure 7.   Range migration of the ground track resulting from earth rotation during the imaging period is shown in a.   The range skew distance is given by $d_r = V_e \cdot \Delta t$ where V_e is the velocity of the earth and Δt is the imaging time for the frame.   The cross track skew shown in b is applied during the image formation.
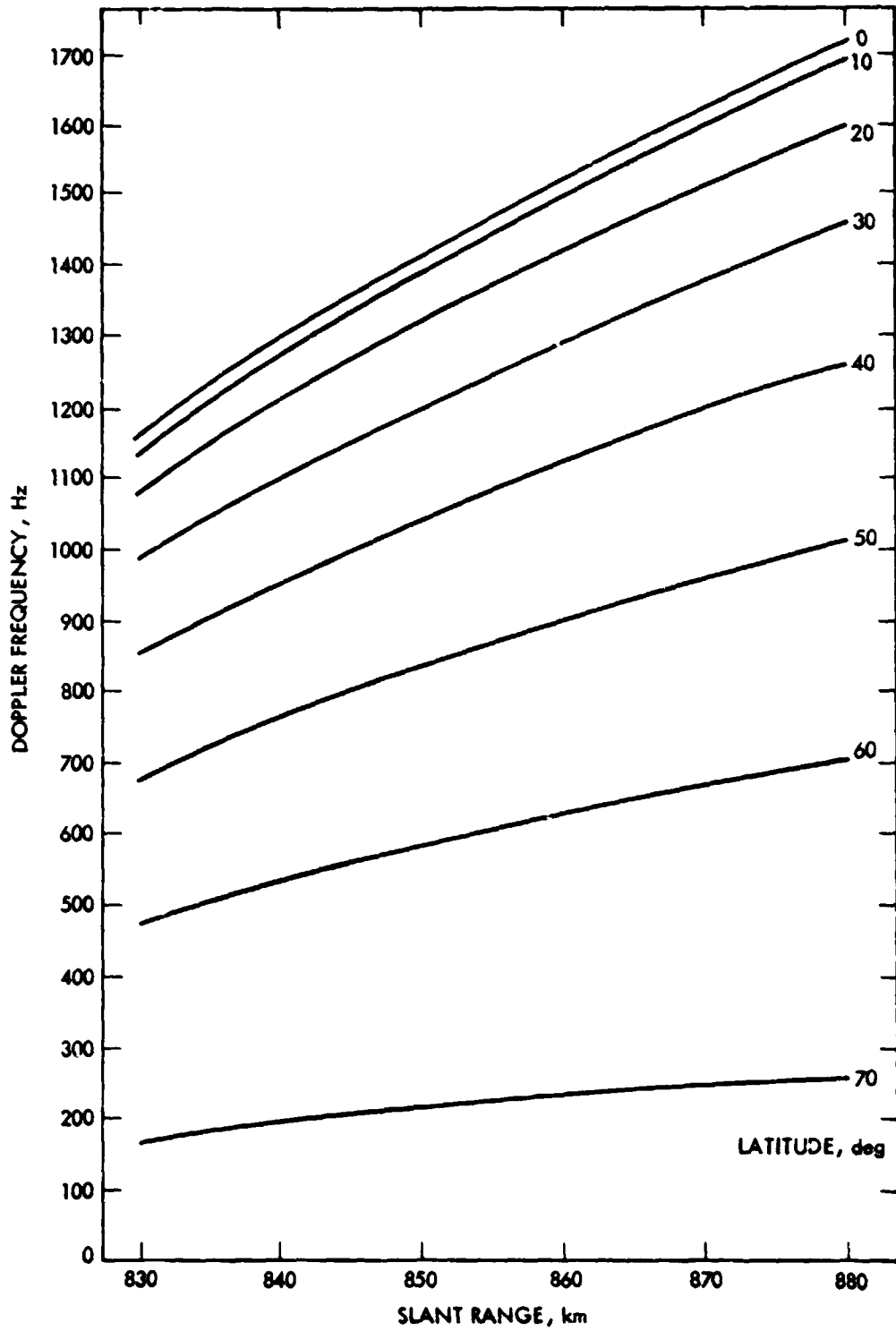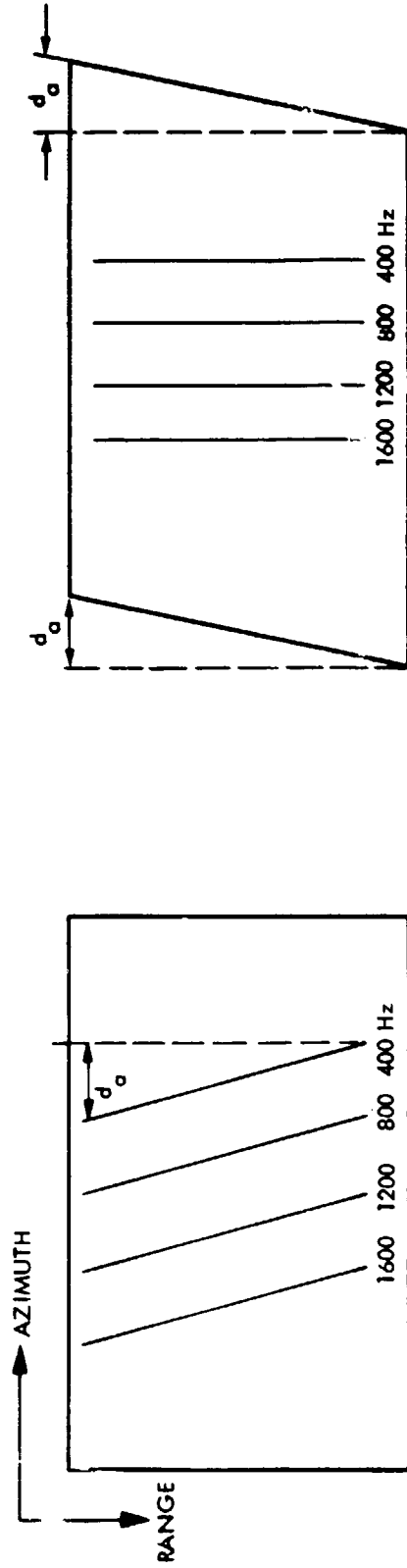
Figure 8. Plot of Doppler frequency as a function of
swath position and latitude. Nominal values
for SEASAT SAR were assumed for spacecraft
in descending mode (Wu, 1981).

193

Figure 9. Azimuth skew resulting from Doppler frequency mismatch during processing. a) Image frame without azimuth skew illustrating orientation of iso-Doppler lines. b) Skewed image showing azimuth displacement d_a. Note: Processor assumes uniform f_d across swath resulting iso-Doppler lines aligning with cross-track direction.

194
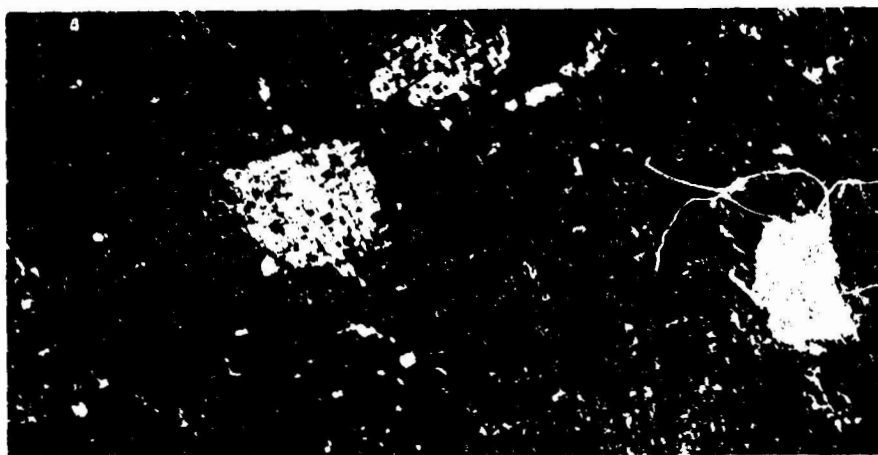
a
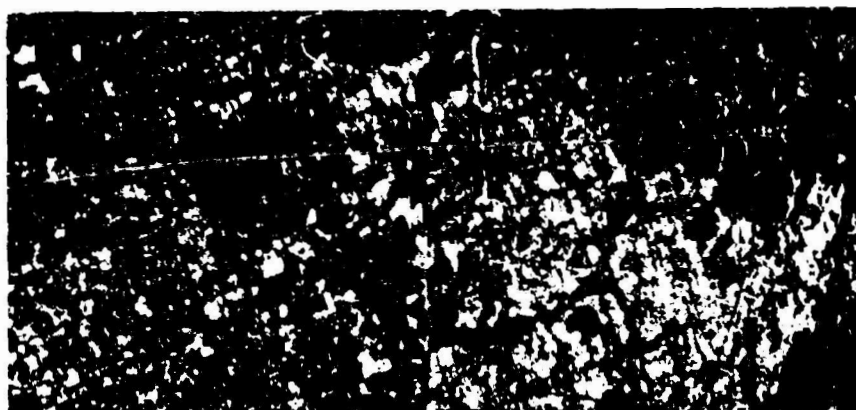
b

Figure 10.   Effect of radar aspect angle on the apparent
brightness of target.   Figure 10a was imaged
during a descending mode and Figure 10b during
an ascending mode
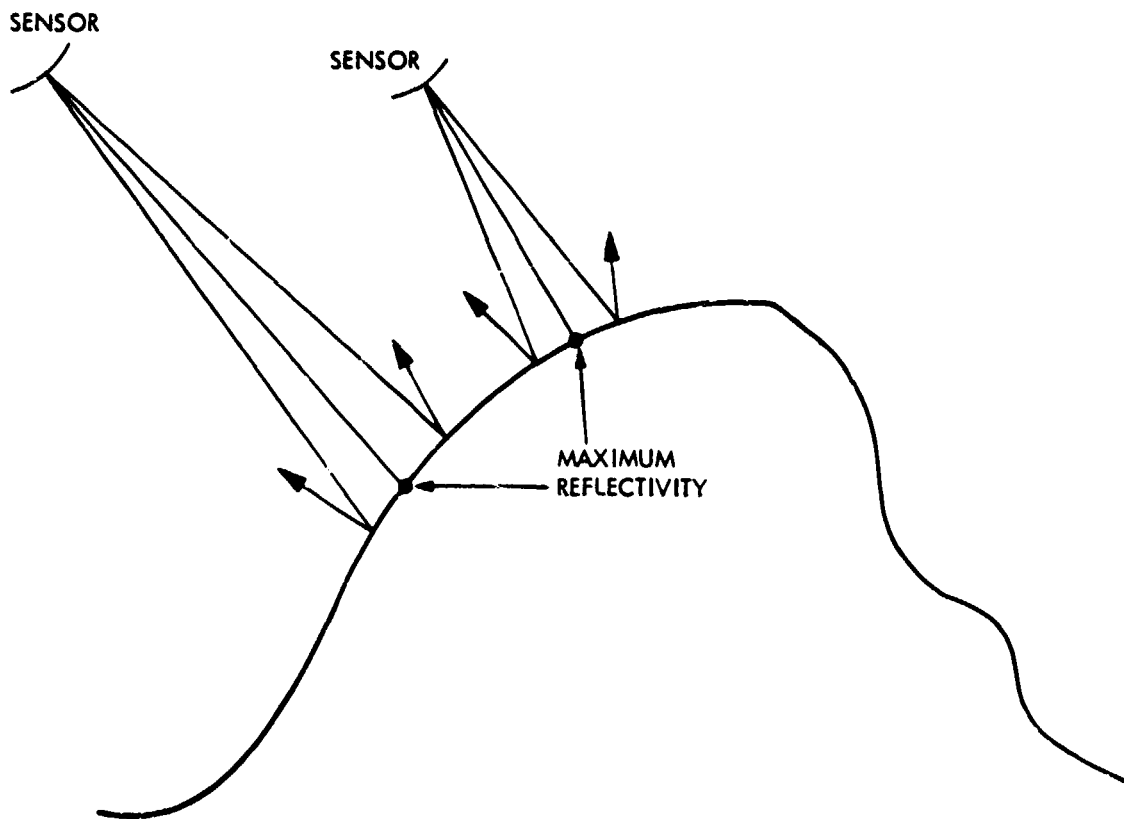
195

SENSOR

SENSOR

MAXIMUM
REFLECTIVITY

Figure 11.   Specular point migration results when sensor images
the same feature from two different positions.
Point of maximum return is dependent on target slope
and may vary relative to other features within the
fra e.

FIBER-OPTIC LINK

HDDT

SEL 32/77
HOST COMPUTER

INTERFACE

SEL BUS

DATA DISK 1

DATA DISK 2

SYSTEM DISK
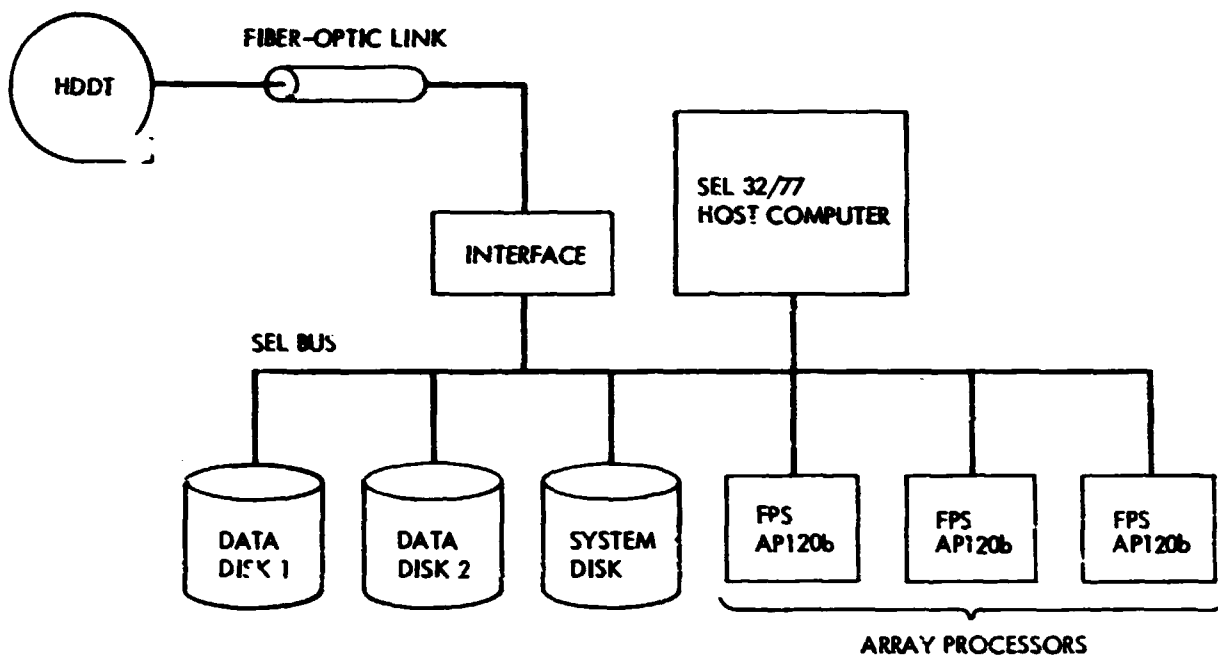
FPS AP120b

FPS AP120b

FPS AP120b

ARRAY PROCESSORS

Figure 12. Block diagram of digital processing system at
Jet Propulsion Laboratory. Data is recorded
on high density digital tape (HDDT) at the
tracking station. It is received at the
processing facility via an optical link and
recorded on disk for processing (Wu, 1981).

197